PHYSICAL REVIEW B VOLUME 14, NUMBER 3 1 AUGUST 1976

Experimental study on the energy loss in argon of ^{252}Cf fission fragments

M. Forte
Physics Division, Centre Commun de Recherche Euratom, Ispra, Italy

A. Bertin, M. Bruno, G. Vannini, and A. Vitale
Istituto di Fisica dell'Università di Bologna and Istituto Nazionale di Fisica Nucleare, Sezione di Bologna, Bologna, Italy

(Received 21 April 1975)

We report the results of a measurement on the energy loss in argon of ^{252}Cf fission fragments having selected masses and initial energies. The experiment was performed with an apparatus combining solid-state and gas-ionization-chamber techniques, which allowed us to study energy-loss characteristics in the range where electronic stopping is dominant. The results for twenty different selected mass intervals are presented and discussed.

I. INTRODUCTION

Since the early work by Rutherford and Bragg,[1] the penetration of energetic charged particles through matter has been continuously studied by nuclear physicists; however, for a long time, a major part of the experimental and theoretical work was concerned primarily with light particles, like protons and α particles, at high energies.

More recently, much interest has been raised on the slowing down of heavy ions in matter, in connection with the development of accelerators which make these particles available with energies up to several MeV amu^{-1}. The demand for more accurate and systematic information concerns, principally, the range and the stopping power for potentially all ions and a great variety of stopping materials.

Energy-loss mechanisms are not essentially different for light and heavier ions; however, the importance of certain phenomena can be very different, in relation with the atomic number Z and the velocity v of the ion in the material medium. In particular, the variation in the ion charge by capture and loss of orbital electrons controls the loss of energy of heavy ions at moderate velocities, while effects of the same kind are not relevant for the slowing down of very light ions like hydrogen or helium.

In current theories, the treatment of the energy-loss mechanism for ions of different atomic numbers is unified, referring to a reduced ion velocity, that is the ratio of the ion velocity, v, to the velocity of electrons in the ion, u. According to Bohr,[2] e.g., the probability itself of capture of an electron by an ion moving in a given material medium is determined by the reduced ion velocity.

In the high-velocity regime,[3] $\xi_k = v/u_k \gg 1$, where u_k is the orbital velocity of k electrons for an ion of atomic number Z, the ion is stripped of all electrons as it penetrates through the absorber material. The transfer of energy of this particle to electrons of the absorber atoms (ionization and excitation) is appropriately described by the Bethe-Bloch theory[4] with suitable corrections,[5] which gives approximately a linear dependence of such *electronic stopping power* on z^2/v^2.

As the ion velocity decreases to values $\xi_k \approx 1$, electrons become attached to the ion and the stopping-power curve falls off the Bethe-Bloch curve. At these velocities, the charge state of the traveling ion can be better described in terms of an effective charge, which depends on the ion velocity, and is no longer an easily observable parameter.[6]

For lower ion velocities ($\xi_k < 1$), several theoretical attempts were achieved to describe the slowing-down process,[7-9] although now none of these seem to be entirely satisfactory.[6] In view of this situation, and with the aim of providing a semiempirical frame to the experimental data, it is currently accepted[10] that the slowing-down process of these ions can be described in the range of moderate velocities by means of range-energy relations with empirically adjustable parameters.

A typical approach along this line is to exploit the simple relations provided by the theory of Lindhard *et al.*[8] for the electronic stopping power (LSS theory), such as

$$x = -h\{[E_0 - \Delta E(x)]^{1/2} - (E_0)^{1/2}\}, \tag{1}$$

where E_0 is the initial particle energy, $\Delta E(x)$ is the energy lost in a path x of a given material, and h is given by

$$h = \frac{\sqrt{2M_1} A_2 v_0 (Z_1^{2/3} + Z_2^{2/3})^{3/2}}{Z_1^W 8\pi e^2 a_0 Z_1 Z_2}, \tag{2}$$

where W is of the order of $\frac{1}{6}$,[8] a_0 and v_0 are the radius and velocity of the first Bohr orbit of hydrogen, e is the electron charge, M_1 and Z_1 are the rest mass and the nuclear charge of the moving ion, and Z_2 and A_2 are the atomic number and atomic weight in grams of the stopping material.

Even if the LSS equation (1) is not correct[6] in its original formulation, it has been advanced[10,11] that it can be quite adequate to represent the results of experiments in the limit of heavy-ion masses if one parameter (either W or h) is considered as adjustable. A procedure of this type will be used to analyze the data of the present work.

Finally one has to remember that, besides via energy transfer to electrons, the incident particle loses energy by collisions with screened nuclei in the absorber, which mainly take place when the ion is approaching the end of its range. In particular, the *nuclear stopping* becomes the dominant energy-loss mechanism at the lowest velocities, when the ion becomes rapidly neutralized.

From the experimental point of view, in order to improve the present knowledge of the slowing down of heavy ions in matter, some significant contributions can be obtained by determining the range relation for fission fragments. In particular, since a large variety of different masses is supplied by a given fissioning nucleus (see Fig. 1), there is an opportunity to perform a systematical study of the dependence of the range-energy relation on the mass of the moving ions. (As it is known, the masses of fragments released in binary fission events can be determined by standard procedures from the recoil energies of both fragments.[12,13])

Up to this date, the slowing down of fission fragments was studied by several groups, both in solid[14] and in gaseous materials.[15] The apparatus used by these authors, however, did not supply a systematical observation of the fragment masses; in particular, the results obtained with gaseous absorbers could only be referred to the median-light (ML) and median-heavy (MH) products from a given source (see Fig. 1), which are emitted with the highest probabilities.

We have performed some systematic measurements on the energy loss of ^{252}Cf fission fragments using gaseous argon as the absorber.

The experiment was carried out by an apparatus providing the following information for each detected fragment: (a) the fragment initial energy (E_0), and (b) the energy loss $\Delta E(x)$ as a function of the range x.

The kinetic energies of the recoiled fragments were measured in coincidence, so that the fragment masses could be calculated off line starting from the kinetic-energy values. The main goals of the experiment were the following: (i) to single out the dependence of the energy-loss characteristics on the mass of the moving fragments for a wide range of masses, (ii) to compare the observed energy-loss curves for fragments having selected energies, and (iii) to explore the possibility of describing the present range-energy data in a semiempirical way, by using Eq. (1) with suitable parametrizations. (Note that the fission fragments from ^{252}Cf are emitted with velocities of about 10^9 cm sec^{-1}, i.e., in the range $\xi_k < 1$; e.g., $\xi_k < 0.7$ for the lightest ones.)

As a final comment to procedure (iii), one may note that, in the limits within which W is constant, one could alternatively exploit Eq. (2) to obtain a determination of the most probable nuclear charge of fission fragments, by observing their masses and energy-loss characteristics.

Some partial results of the present work have already been published.[11] Here we report the results of more extended observations, giving a detailed account of the measurements (Sec. II) and of the analysis of the data (Sec. III).

II. EXPERIMENT

A. Apparatus

The experiment was performed using an apparatus which was fully described elsewhere[16]; here

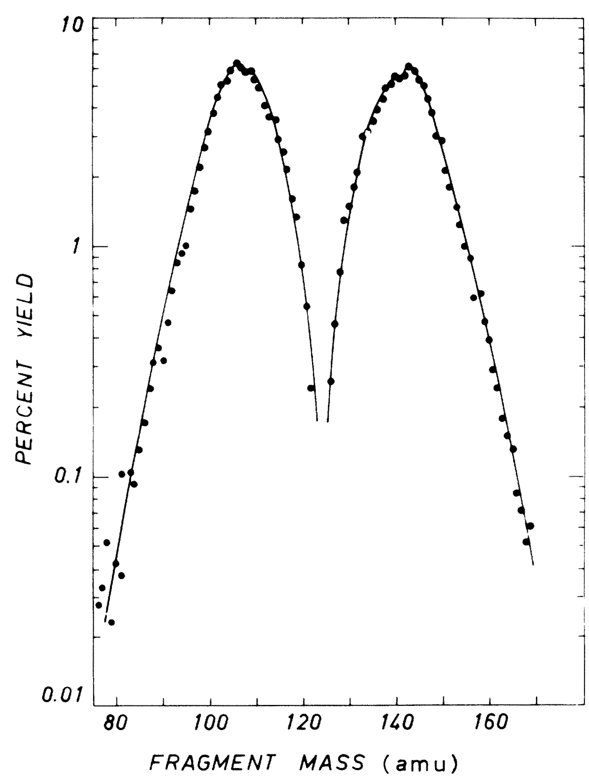

FIG. 1. Percent yield of fission fragments from ^{252}Cf as a function of the mass number (postneutron emission values).

we shall only restate the principle of its operation, together with some of its main characteristics.

A weightless source of ^{252}Cf was mounted between two opposite solid-state detectors (S_1 and S_2, see Fig. 2) within a stainless-steel vessel (V) containing gaseous argon at subatmospheric pressure. The source was prepared by the self-transfer technique,[17] and supplied about 250 fission events per sec over the whole solid angle. The fragments owing to a binary fission event, recoiling in opposite directions along the distances d_1 and d_2, and loosing part of their energy in the gas, were finally stopped within S_1 and S_2, which measured in coincidence their residual energies $E(S_1)$ and $E(S_2)$ (S_1 and S_2 were 1 cm^2 sensitive area, 290-Ω cm n-type silicon detectors).

Two sections of the ionization chamber (A_1 and A_2), in detecting the ionization produced in the gaseous absorber[18] measured the energies $E(A_1)$ and $E(A_2)$ lost by the fragments along d_1 and d_2, respectively. In such a way, the original kinetic energies $E_{0,1}$ and $E_{0,2}$ of the fragments $[E_{0,i} = E(A_i) + E(S_i)]$ could also be reconstructed.

The electrostatic design of the ionization chamber was such that the anodes A_1 and A_2 could collect only the electrons released by the ionizing fragments along d_1 and d_2, respectively. To avoid distortions of the electric field in the neighborhood of the source, its (10 μg cm^{-2}) Vyns backing was covered with an additional (10 μg cm^{-2}) layer of evaporated gold, and held at earth potential. In these conditions, the MH and ML fragments from ^{252}Cf were losing less than 1% of their initial kinetic energies while crossing the source's backing.[19]

Figure 2 shows a block diagram of the electronics. The pulses from A_1, A_2, S_1, and S_2 were amplified by low-noise charge-sensitive electronics,[20] and finally sent to 1000 channels analog-to-digital converters (ADC). The signals from S_1 and S_2 were separately sent to a coincidence circuit, which supplied a gating signal for the integrating amplifiers (I.A.), in order to select those pulses owing to one binary fission event. The digitalized outputs from the ADC's were sent to scalers, and finally recorded on magnetic tape for the off-line analysis. For such a purpose each detected fission event was defined by the four digitalized values of the signals from A_1, A_2, S_1, and S_2.

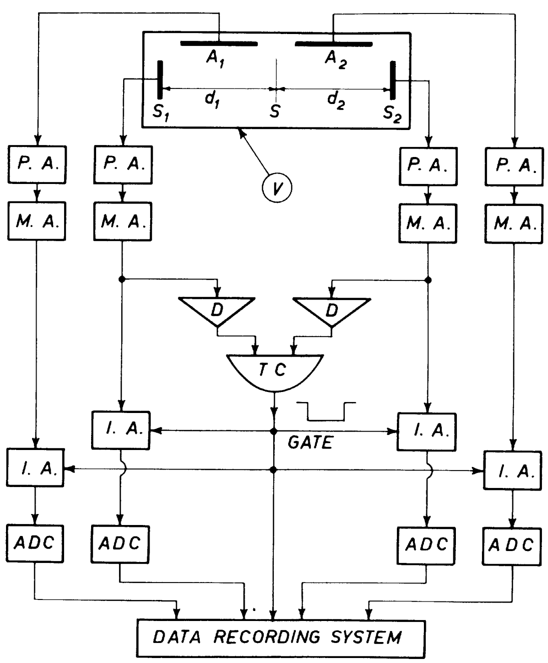

FIG. 2. Simplified scheme of the apparatus and block-diagram of the electronics. V, gas vessel; A_1, A_2, ionization chamber anodes; S_1, S_2, solid-state detectors; S, weightless source of ^{252}Cf; P. A., preamplifiers; M. A., main amplifiers; I. A., integrating amplifiers; D, discriminators; TC, trigger coincidence; ADC, analog-to-digital converters.

B. Measurements

The data were taken performing a high-statistics run for each selected value of the gaseous range. On the whole, about 2×10^6 fission fragments were observed.

The gaseous path which the recoiling fragments crossed before reaching S_1 or S_2 was varied by changing the pressure of the gas, and keeping d_1 and d_2 at fixed values. The pressure was varied from a minimum value of 20 Torr up to maximum values of about 200 Torr; the minimum distance at which the solid-state detectors were set from the source of ^{252}Cf was 5 cm. Keeping into account the accuracy with which the pressure was measured (0.5 Torr), and the geometry of the source and detectors, the measured ranges were affected by a maximum error of about 3%, which was reduced to 1% for the highest-pressure values.

Part of the measurements were carried out by setting S_1 and S_2 in symmetrical positions with respect to the source ($d_1 = 5$ cm $= d_2$), and increasing the pressure in steps $\Delta p = 10$ Torr. In these conditions, however, since the heavy fragments have shorter total ranges than their light partners, the chosen coincidence technique would compel one to stop observing the light fragments when they are still far from the end of their range in argon. To overcome this limitation, some measurements were carried out by setting S_1 and S_2 in asymmetrical positions ($d_1 = 7.5$ cm, $d_2 = 5$ cm, $\Delta p = 6.7$

Torr); in this way, the whole mass spectrum of fragments belonging to the light group could still be observed in S_1, while the mass distribution of the heavy fragments detected by S_1 was progressively reduced at increasing pressure (see Fig. 3).

The runs were carried out in steps of 5000 binary fission events at a time. These measurements were alternated with auxiliary runs, which were performed keeping the chamber evacuated and working with S_1 and S_2 only (*vacuum runs*). The *vacuum runs* were carried out before each filling operation at a given pressure, also recording 5000 fission events per run. As explained later on, these measurements were necessary to match the energy scale of the ionization chambers to the one of the solid-state detectors.

Other reference measurements were periodically performed to check the working conditions of S_1, S_2, A_1, and A_2, as well as the integrity of the source, by recording the spectra of the 6.13-MeV α particles from ^{252}Cf separately in each section

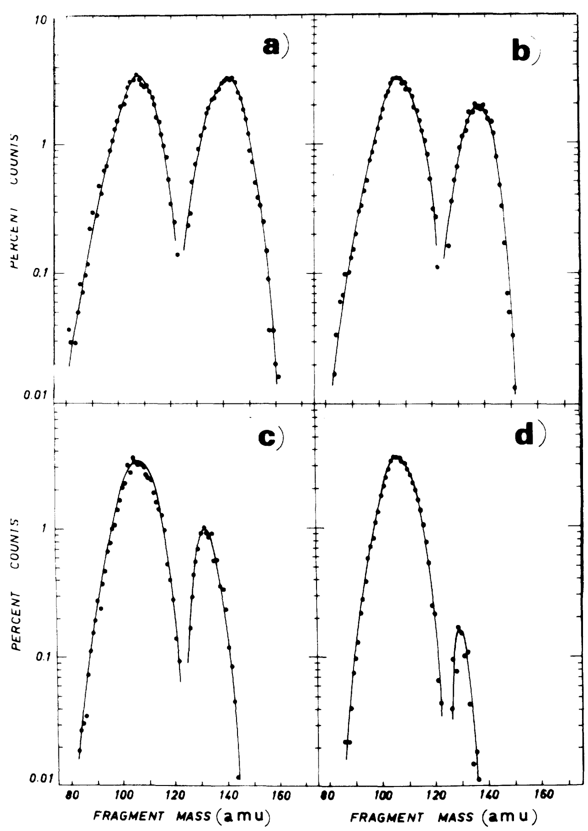

FIG. 3. Mass distribution of the fission fragments detected by S_1 for increasing gaseous ranges. Ordinates are normalized to twice the area of the peak of the light group. Data were taken setting $d_1 = 7.5$ cm, $d_2 = 5$ cm, the pressure was set equal to (a) 120 Torr; (b) 13.3 Torr, (c) 14.7 Torr, (d) 160 Torr.

of the apparatus. The energy resolution of S_1 and S_2 for these particles was better than 1% (full width at half maximum); the amplitude distribution of the sum of the signals released by A_1 and S_1 (A_2 and S_2) for the same particles showed a resolution better than 1.5%.

C. Data processing

As already specified, each of the fission events recorded under pressure was defined by four recorded amplitudes (A_1, S_1, A_2, S_2) which had to be treated to obtain the energy values $E(A_1)$, $E(A_2)$, $E(S_1)$, and $E(S_2)$. (Remember here that the observed energies were postneutron emission values; neutron emission, in fact, occurs in a time of the order of 10^{-17} sec after scission.)

For this purpose, it is necessary to know the mass dependence of the pulse height versus energy relation for the chosen detectors. Since the energy response of the semiconductor ion detectors was accurately established by Schmitt *et al.*,[21] it was decided to match the energy scale of the ionization chamber sections to the one of S_1 and S_2. This was done run by run, for each section $(i = 1, 2)$ of the apparatus, starting from the observed amplitude distribution of the *sum of the signals* released from the ionization chamber and from the solid-state detector $[(A_i + S_i)$ distribution]; and looking for a correction function C_i such that the distribution of the *corrected* amplitudes $T_i = (C_i \times A_i) + S_i$ overlapped with the amplitude spectrum $(S_{V,i})$ precedingly recorded during the *vacuum run*.[16] Pushing the overlapping procedure until the ML and MH peaks of the T_i distribution coincided with those of the $S_{V,i}$ spectrum within 1%, it turned out that: (a) the C_i's were determined with an average accuracy better than 2%, and (b) for each section of the apparatus, C_i was practically independent of the gaseous pressure (within the range explored) and of the fragment mass.

Once the C_i factors were determined, *each event* was defined by four amplitudes, i.e., $C_1 \times A_1$, S_1, $C_2 \times A_2$, and S_2. To express these amplitudes in terms of energy T_1 and T_2 were considered as two signals entirely released from S_1 and S_2, and the post-neutron emission values for the total energies $E_{0,1}$ and $E_{0,2}$ and masses M_1 and M_2 were calculated starting from T_1 and T_2 by a usual iteration procedure,[13] which includes the mass-dependent energy calibration by Schmitt *et al.*,[21] as well as the corrections owing to the neutron emission based on the results by Bowman *et al.*[22] and by Terrell.[23] The computation process was repeated until the difference in the mass values resulting from two consecutive iterations was less than 0.1%. In the average, not more than four iterations were required for convergence.

In conclusion, four items of information were associated with each detected *fragment*: the total initial energy E_0, the amplitudes $C \times A$ and S [from which the energy $E(A)$ lost in the gas and the residual energy $E(S)$ could now be obtained], and the fragment mass M.

As to the accuracy of this procedure, one has to say that two different sources of uncertainty are present: first, the instrumental effects and intrinsic detector resolution; and, second, the energy dispersion which is due to the varying energy and number of emitted neutrons. The usual way of removing the overall dispersion is the *folding procedure* proposed by Terrell;[23] however, it was shown[13,24] that the iterative method used in the present work has the same resolving effect of the folding procedure. Therefore, the usual dispersion correction was assumed to be unnecessary. Since the overall instrumental error in the measured kinetic energies of the fission fragments was estimated to be less than 2%, the reconstructed values of the fragment masses are considered accurate to within ±1 amu. As a result of the whole treatment, it was verified that the energy distribution, the mass spectrum, and the energies of the fragments having a given mass were practically the same as those obtained from the events recorded during the vacuum runs.

III. RESULTS AND DISCUSSION

The data obtained as described above were treated by the following criteria: (i) having in mind the uncertainty of ±1 amu in the determination of the fragment masses, the observed fragments were first grouped into three-mass intervals for the subsequent analysis, as is shown in Table I. (ii) The distribution of the initial energies E_0 for fragments belonging to the different mass intervals was reconstructed from the collected events (see Fig. 4). It appears from this figure that the fragments of the heavy group have initial energies which are more mass dependent than those of the light group. The average values of the initial energies $\langle E_0 \rangle$ for each mass interval are listed in Table I. (iii) The average energy loss $\Delta E(X)$ in a gaseous path x for fragments belonging to a given mass interval, and for chosen initial energies, was determined by the centroid of the histogram of the corresponding energy losses. According to the statistics collected, the average $\Delta E(X)$ values were always determined with an accuracy better than 0.5 MeV. (iv) Finally, these results were compared with Eq. (1).

As said previously the heavy ions also lose energy by nuclear collisions, so that a complete treatment of their moderation in matter should take into account both the electronic and the nuclear stopping power. However, it has been shown by Lindhard *et al.*[8] that the nuclear collisions contribute effectively to the stopping when

TABLE I. Average values $\langle E_0 \rangle$ of the observed initial energies for ^{252}Cf fission fragments belonging to different mass intervals.

Curve No. [a]	Mass interval (amu)	$\langle E_0 \rangle$ (MeV)
1	93–95	105.6
2	96–98	105.4
3	99–101	105.4
4	102–104	105.2
5	105–107 [b]	104.1
6	108–110	102.6
7	111–113	101.1
8	114–116	100.1
9	117–119	98.2
10	120–122	93.6
11	126–128	92.1
12	129–131	91.3
13	132–134	88.1
14	135–137	85.3
15	138–140	81.9
16	141–143 [c]	79.3
17	144–146	75.7
18	147–149	72.2
19	150–152	68.5
20	153–155	64.7

[a] Quoted for reference to Fig. 4.
[b] Interval centered on the ML fragment mass.
[c] Interval centered on the MH fragment mass.

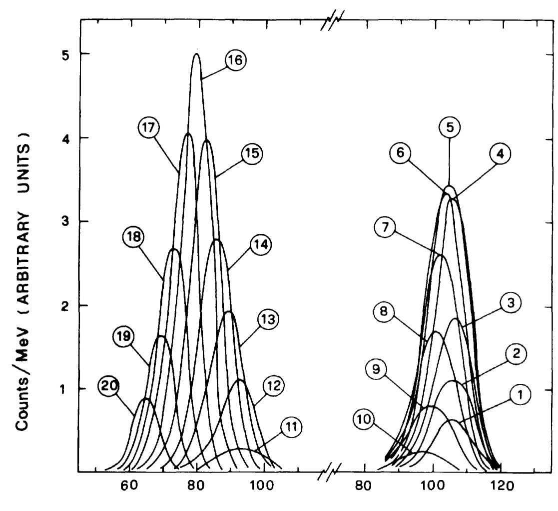

FIG. 4. Initial energy distributions for ^{252}Cf fission fragments belonging to different mass intervals. Curves 1–20 refer to the mass intervals indicated in Table I.

the ion is approaching the end of its range, whereas they occur at negligible rate for small values of the range. In particular, using the formulas by Lindhard *et al.*,[8] one may easily see that the nuclear stopping power for the MH fragments of ^{252}Cf is about 10% of the electronic one at a range of 1.9 mg/cm^2 in argon.

With this in mind, the comparison of the present experimental results to the LSS equation (1) was limited to that part of the range in which the nuclear stopping power is predicted to be less than 5% of the electronic one (e.g., to $x = 1.3$ mg/cm^2 for the MH fragments and to $x = 2.1$ mg/cm^2 for the ML fragments).

The present data were fitted to Eq. (1) in two independent ways: (a) considering first the quantity h as a free parameter, and (b) leaving W as a free parameter. In the latter case, the correspondence between Z and M was assumed from the experimental results by Reisdorf *et al.*[25] The results obtained will now be discussed in detail.

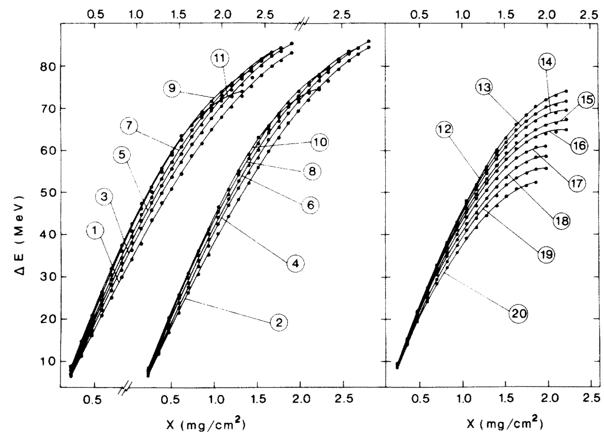

FIG. 5. Average energy loss ΔE of fission fragments along their range in argon. Full circles, experimental points. Curves refer to mass intervals and initial energies as listed in Table I (the energies were selected within the range $\langle E_0\rangle \pm 1$ MeV).

A. Energy loss for fragments having their most probable initial energy

For each of the mass intervals listed in Table I, only the fragments carrying their most probable initial energy $\langle E_0\rangle \pm 1$ MeV were considered at first. The average energy losses $\Delta E(x)$ obtained for these fragments as a function of the gaseous range x are shown in Fig. 5 and listed in Tables II and III. It is seen from Fig. 5 that all fragments

TABLE II. Observed energy loss in argon [$\Delta E(x)$] of ^{252}Cf fission fragments having selected masses *(light fragments)* and initial energies.[a]

x (mg/cm^2)	Mass interval (amu) 93–95	96–98	99–101	102–104	105–107	108–110	111–113	114–116	117–119	120–122
	$\Delta E(x)$ (MeV)									
0.23	6.8	6.9	7.3	7.5	7.7	7.9	8.1	8.3	8.5	8.6
0.35	11.5	12.0	12.3	12.6	12.9	13.3	13.6	13.7	14.2	13.9
0.47	16.3	17.0	17.3	18.0	18.5	18.8	19.3	19.8	19.9	20.5
0.59	21.0	21.7	22.3	22.9	23.5	24.0	24.6	25.1	25.6	25.9
0.70	25.2	26.4	26.9	27.8	28.3	28.8	29.6	30.0	30.7	31.0
0.82	30.1	30.9	31.8	32.7	33.4	34.1	34.7	35.3	36.2	36.3
0.94	34.2	35.4	36.4	37.5	38.2	39.0	39.7	40.4	41.0	41.5
1.05	38.0	40.4	41.6	42.7	43.4	44.3	44.9	45.6	46.4	46.7
1.17	43.6	44.5	46.0	47.1	47.8	48.6	49.0	49.6	50.3	50.9
1.29	47.7	48.5	50.0	51.2	51.9	52.9	53.5	54.4	55.1	55.2
1.41	51.0	52.4	53.9	54.9	55.8	56.6	57.5	58.3	59.2	59.3
1.52	54.6	56.1	57.4	58.4	59.4	60.3	61.1	61.9	62.8	63.3
1.64	58.9	60.1	61.7	62.7	63.5	64.4	65.0	66.0	66.3	65.4
1.76	61.9	63.2	64.5	65.7	66.4	67.3	68.1	68.8	69.3	68.3
1.87	65.2	66.7	67.9	69.0	69.7	70.4	70.9	71.5	72.0	70.5
1.99	68.2	69.5	70.8	71.8	72.5	73.1	73.6	74.3	74.2	72.3
2.11	70.7	72.1	73.2	74.4	74.7	75.8	75.9	76.4	76.2	73.3
2.23	73.1	74.8	75.8	76.8	77.4	78.0	78.2	78.2	77.7	75.1
2.34	75.6	76.8	77.9	78.7	79.2	79.5	79.7	79.9	79.4	
2.46	78.1	79.4	80.4	81.3	81.6	81.7	81.8			
2.58	80.2	81.3	82.6	83.1	83.4	83.6	83.4			
2.69	81.6	82.9	83.7	84.3	84.5	84.2				
2.81	83.3	84.4	85.5	86.0						

[a] For each mass interval, only the fragments having initial energy $\langle E_0\rangle \pm 1$ MeV were selected, the correspondence between $\langle E_0\rangle$ and fragment masses being given in Table I.

TABLE III. Observed energy loss in argon [$\Delta E(x)$] of ^{252}Cf fission fragments having selected masses *(heavy fragments)* and initial energies.[a]

x (mg/cm^2)	Mass interval (amu) 126–128	129–131	132–134	135–137	138–140	141–143	144–146	147–149	150–152	153–155
	$\Delta E(x)$ (MeV)									
0.23	9.1	9.2	9.4	9.5	9.5	9.4	9.2	9.0	8.9	8.6
0.35	14.9	15.5	15.6	15.6	15.6	15.5	15.2	14.9	14.5	14.0
0.47	21.0	21.7	21.8	21.9	21.7	21.6	21.2	20.7	20.1	19.5
0.59	26.6	27.4	27.5	27.4	27.3	27.1	26.6	26.0	25.0	24.2
0.70	32.2	32.7	32.8	32.9	32.4	32.0	31.4	30.5	29.5	28.4
0.82	37.7	38.1	38.1	38.0	37.4	36.9	35.9	34.9	33.7	32.3
0.94	42.7	42.9	42.8	42.5	41.8	41.2	40.1	38.8	37.5	35.8
1.05	47.6	48.1	47.8	47.3	46.3	45.4	44.1	42.6	41.0	39.1
1.17	51.5	51.9	51.5	50.8	49.6	48.6	46.9	45.2	43.9	41.7
1.29	55.9	56.2	55.4	54.6	53.3	52.2	50.5	48.6	46.8	44.5
1.41	59.7	60.1	59.1	58.0	56.5	55.1	53.3	51.3	49.2	46.8
1.52	63.7	63.1	62.1	60.9	59.5	58.0	56.1	53.6	51.8	49.1
1.64	66.2	66.2	64.9	63.6	61.8	60.4	58.3	56.0	53.5	50.9
1.76	68.6	68.4	67.0	65.6	63.6	62.0	59.6	57.2	54.6	51.7
1.87	70.4	70.5	68.7	67.1	65.0	63.3	60.8	58.4	55.6	52.5
1.99	72.1	72.1	70.4	68.3	66.1	64.0	61.0	58.6	55.7	
2.11	73.1	73.2	70.9	69.0	66.6	64.5				
2.23	74.4	74.2	71.8	69.7	67.4	65.0				

[a] For each mass interval, only the fragments having initial energy $\langle E_0 \rangle \pm 1$ MeV were selected, the correspondence between $\langle E_0 \rangle$ and fragment masses being given in Table I.

belonging to the heavy group show a trend to reach flat tops at the largest x values, and that also the heaviest fragments (curves 9 and 10) of the light group present a similar behavior. This fact indicates that these fragments are approaching the end of that part of the range where the electronic stopping is effective.

Fitting the first part of each of these curves to Eq. (1), the two parameters h and W considered separately were extracted out. The results of these fitting procedures are reported in Table IV and represented in Fig. 6 as a function of the fragment mass. It appears that h and W depend almost linearly on the fragment mass up to about $M = 135$ amu, reaching thereafter a sort of plateau. Such a behavior first confirms that the LSS theory is inadequate to reproduce the observed energy-range curves for a wide range of fragment masses. On the other hand, even if very heavy fragments h and W seem to be constant (although different from the values foreseen by the LSS theory, e.g., $W=\frac{1}{6}$), one has to remember that the results shown in Fig. 6 refer to different initial energies as well as to different mass intervals.

Therefore, the data were further analyzed by two different approaches, in order to give separate evidence for the dependence of the energy-loss characteristics on the fragment mass and initial energy.

TABLE IV. Values of the parameters h and W obtained by fitting the range-energies curves of Fig. 5 to Eq. (1). The errors presented on h and W are those supplied by the fitting procedure. These results are plotted in Fig. 6 as a function of the fragment masses.

Mass interval (amu)	h (mg cm^{-2} MeV$^{-1/2}$)	W	χ^2/N_{DF}
93–95	0.364 ± 0.003	0.268 ± 0.002	1.31
96–98	0.355 ± 0.002	0.274 ± 0.002	1.32
99–101	0.345 ± 0.002	0.280 ± 0.002	1.39
102–104	0.335 ± 0.002	0.286 ± 0.002	1.17
105–107	0.328 ± 0.002	0.291 ± 0.002	1.25
108–110	0.316 ± 0.002	0.299 ± 0.002	0.95
111–113	0.308 ± 0.002	0.304 ± 0.002	0.87
114–116	0.301 ± 0.002	0.306 ± 0.002	1.22
117–119	0.293 ± 0.002	0.315 ± 0.002	1.42
120–122	0.278 ± 0.002	0.328 ± 0.002	1.16
126–128	0.273 ± 0.002	0.331 ± 0.002	1.59
129–131	0.270 ± 0.002	0.333 ± 0.002	1.00
132–134	0.266 ± 0.002	0.338 ± 0.002	1.01
135–137	0.263 ± 0.003	0.342 ± 0.003	0.93
138–140	0.264 ± 0.003	0.339 ± 0.003	1.32
141–143	0.262 ± 0.003	0.341 ± 0.003	1.19
144–146	0.261 ± 0.004	0.341 ± 0.004	1.36
147–149	0.264 ± 0.004	0.337 ± 0.004	1.60
150–152	0.261 ± 0.005	0.339 ± 0.005	0.53
153–155	0.266 ± 0.005	0.333 ± 0.005	0.77

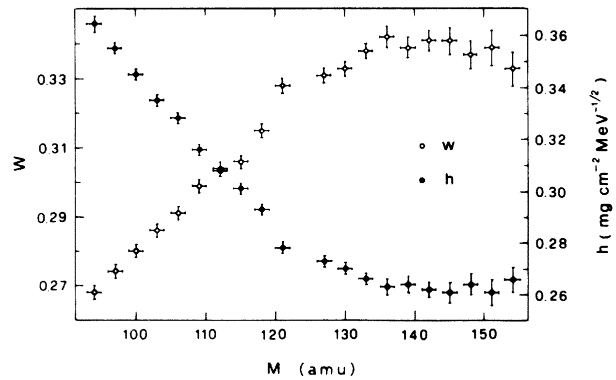

FIG. 6. Values of the parameters h and W obtained by fitting the range-energy curves in Fig. 5 to Eq. (1) as a function of the fragment mass.

B. Energy loss of fragments having the same initial energy

The broad initial energy distributions observed for the ^{252}Cf fission fragments (see Fig. 4) allow one to consider several fragments having different masses but the same initial energy. As a second step of the analysis, therefore, the energy loss of fragments having different masses was determined as a function of range, selecting fragments with the same initial energy $E_0 = 104.1 \pm 1$ MeV (for the light group) and $E_0 = 79.3 \pm 1$ MeV (for the heavy group).

The value of the initial kinetic energies being fixed, this type of analysis provides a direct observation of the dependence of the energy-range curves on the fragment mass. The results obtained are presented in Fig. 7 and listed in Tables V and VI, and seem to indicate that light fragments and heavy fragments lose energy through somewhat different mechanisms. The energy loss of the fragments of the light group [see Fig. 7(a)] is in fact mass dependent, i.e., for a given gaseous path $\Delta E(x)$ increases with mass. On the other hand, the range-energy curves of the fragments belonging to the heavy group are almost coincident [Fig. 7(b)]. The fact that even in this case small differences are actually present in the last part of the observed range can qualitatively be explained in terms of nuclear scattering, which begins to be significant in this region.

The results of fitting the first part of these energy-range data with Eq. (1) are reported in Table VII, and the values obtained independently for h and W are shown in Fig. 8. It is seen from these data that, for the present absorbing medium and for fragments having the given initial energies, Eq. (1) reproduces the present results for very heavy ions, provided the experimental value W

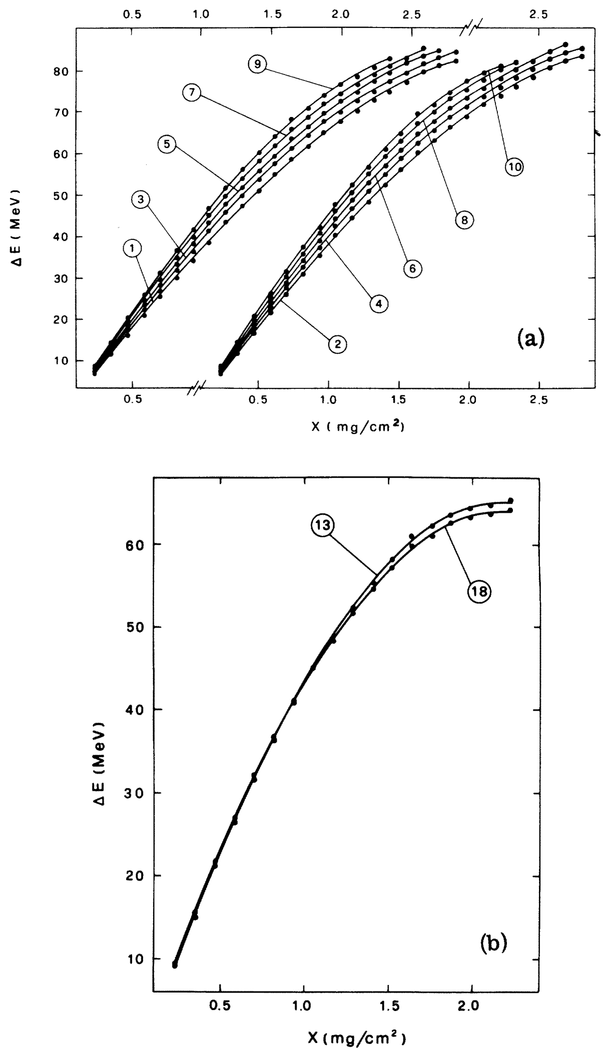

FIG. 7. Average energy loss (ΔE) of fission fragments having the same initial kinetic energy, i.e.; (a) $E_0 = 104.1 \pm 1.0$ MeV, and (b) $E_0 = 79.3 \pm 1.0$ MeV. Curves refer to mass intervals as listed in Table I. As to curves in (b), only curves 13 and 18 are presented, since the intermediate ones fall within them.

$= 0.340$ is assumed. The corresponding value for h is 0.263 mg cm^{-2} MeV$^{-1/2}$. In other words W and h turn out to be independent of the fragment mass, for the slowing down in gaseous argon of very heavy fission fragments starting with the same kinetic energy.

C. Energy loss of the medium-heavy and medium-light fragments for different initial energies

To complete the present study of the slowing down mechanism of fission fragments in matter, the dependence of the energy loss of fragments of a fixed mass on their initial energy is still to be

TABLE V. Observed energy loss in argon [$\Delta E(x)$] of ^{252}Cf fission fragments having selected masses ***(light fragments)*** and the same initial kinetic energy $E_0 = 104.1 \pm 1.0$ MeV.[a]

	Mass interval (amu)									
	93–95	96–98	99–101	102–104	105–107	108–110	111–113	114–116	117–119	120–122
x (mg/cm^2)	$\Delta E(x)$ (MeV)									
0.23	6.8	6.9	7.3	7.5	7.7	7.9	8.1	8.3	8.5	8.6
0.35	11.5	11.9	12.2	12.6	12.9	13.4	13.6	13.9	14.4	14.5
0.47	16.2	16.9	17.3	17.9	18.5	18.9	19.3	19.8	20.3	20.8
0.59	20.9	21.6	22.3	22.9	23.5	24.0	24.6	25.2	25.9	26.2
0.70	25.5	26.0	26.9	27.7	28.3	28.9	29.7	30.4	31.1	31.7
0.82	30.0	31.0	31.8	32.7	33.4	34.2	34.9	35.8	36.6	37.5
0.94	34.2	35.5	36.4	37.3	38.2	39.0	39.9	40.8	41.6	42.2
1.05	38.5	40.4	41.4	42.5	43.4	44.3	45.2	46.1	46.9	47.9
1.17	43.5	44.6	45.8	46.9	47.8	48.8	49.8	50.7	51.8	52.5
1.29	47.3	48.4	49.9	51.0	51.9	53.0	54.0	55.1	56.1	56.6
1.41	51.2	52.5	53.8	55.0	55.8	57.0	58.1	59.3	60.3	61.0
1.52	55.0	56.2	57.7	58.8	59.4	60.8	61.9	63.0	64.2	64.9
1.64	58.7	60.1	61.4	62.5	63.5	64.7	65.8	67.1	68.2	69.6
1.76	61.7	63.1	64.3	65.5	66.4	67.7	68.7	69.9	70.8	71.7
1.87	65.0	66.4	67.6	68.7	69.7	70.8	72.0	73.1	74.0	74.7
1.99	67.6	68.9	70.0	71.1	72.5	73.3	74.3	75.4	76.6	77.3
2.11	70.2	71.8	72.7	73.7	74.7	75.6	76.7	77.7	78.5	79.3
2.23	72.8	73.7	74.8	75.9	77.4	78.0	78.8	80.1	80.6	81.0
2.34	74.9	76.1	77.3	78.2	79.2	80.2	81.0	82.0	82.9	
2.46	77.2	78.4	79.3	80.3	81.6	82.1	82.9			
2.58	79.7	80.7	81.7	82.6	83.4	84.3	85.2			
2.69	81.1	82.1	83.0	84.1	84.5	86.0				
2.81	82.2	83.4	84.4	85.1						

[a] The average kinetic energy of the median-light fragment is 104.1 MeV (see Table I).

TABLE VI. Observed energy loss in argon [$\Delta E(x)$] of ^{252}Cf fission fragments having selected masses ***(heavy fragments)*** and the same initial kinetic energy $E_0 = 79.3 \pm 1.0$ MeV.[a]

	Mass interval[b] (amu)					
	132–134	135–137	138–140	141–143	144–146	147–149
x (mg/cm^2)	$\Delta E(x)$ (MeV)					
0.23	9.2	9.3	9.3	9.4	9.4	9.4
0.35	15.0	15.2	15.3	15.5	15.5	15.6
0.47	21.2	21.3	21.5	21.6	21.7	21.7
0.59	26.5	26.8	26.9	27.1	27.1	27.0
0.70	31.6	31.7	31.9	32.0	32.1	32.0
0.82	36.4	36.7	36.9	36.9	36.9	36.8
0.94	40.9	41.0	41.1	41.2	41.2	41.1
1.05	45.2	45.4	45.4	45.4	45.2	45.1
1.17	48.8	48.4	48.5	48.6	48.5	48.3
1.29	52.3	52.1	52.3	52.2	52.0	51.7
1.41	55.3	55.2	55.1	55.1	54.8	54.6
1.52	58.2	57.9	57.9	58.0	57.6	57.2
1.64	61.0	60.5	60.4	60.4	60.2	59.8
1.76	62.2	61.7	61.8	62.0	61.4	61.0
1.87	63.6	63.6	63.4	63.3	63.0	62.6
1.99	64.4	64.2	64.1	64.0	63.6	63.3
2.11	64.8	64.2	64.0	64.5	63.5	63.7
2.23	65.4	65.3	65.2	65.0	64.7	64.2

[a] The average kinetic energy of the median-heavy fragment is 79.3 MeV (see Table I).
[b] The mass intervals corresponding to curves 11, 12, 19, and 20 were not considered for the present analysis since the statistics corresponding to the present energy selection was too poor (see Fig. 4).

TABLE VII. Values of the parameters h and W obtained by fitting the curves in Fig. 7 to Eq. (1). The errors on h and W are those supplied by the fitting procedure.

Mass interval (amu)	h ($\mathrm{mg\,cm^{-2}\,MeV^{-1/2}}$)	W	χ^2/N_{DF}
93–95	0.362 ± 0.003	0.270 ± 0.002	1.33
96–98	0.353 ± 0.002	0.276 ± 0.002	1.70
99–101	0.343 ± 0.002	0.281 ± 0.002	1.76
102–104	0.333 ± 0.002	0.288 ± 0.002	1.43
105–107	0.328 ± 0.002	0.291 ± 0.002	1.25
108–110	0.318 ± 0.002	0.298 ± 0.002	1.05
111–113	0.311 ± 0.002	0.302 ± 0.002	1.22
114–116	0.304 ± 0.002	0.304 ± 0.002	1.48
117–119	0.298 ± 0.002	0.311 ± 0.002	1.63
120–122	0.286 ± 0.002	0.320 ± 0.002	0.38
132–134	0.265 ± 0.003	0.338 ± 0.003	1.22
135–137	0.265 ± 0.003	0.341 ± 0.003	1.45
138–140	0.265 ± 0.003	0.338 ± 0.003	1.62
141–143	0.262 ± 0.003	0.341 ± 0.003	1.19
144–146	0.260 ± 0.004	0.342 ± 0.003	1.02
147–149	0.263 ± 0.004	0.338 ± 0.003	1.15

discussed. For this purpose, the range-energy curves for the MH and ML fragments were extracted from the experimental data selecting five different initial energies. These curves are shown in Figs. 9(a) and 9(b), and the corresponding data are reported in Tables VIII and IX.

The parameters h and W obtained from the fitting procedures with Eq. (1) are presented in Fig. 10, and reported in Table X as a function of the initial energy. Such an analysis shows that, for the MH fragments [see Table X(a)] the energy-range relation is very well reproduced by an expression of the type

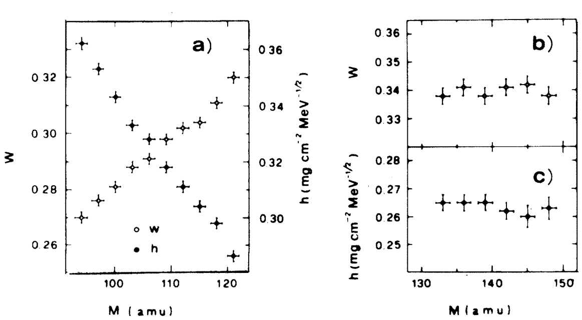

FIG. 8. Values of the parameters h and W obtained by fitting the range-energy curves in Fig. 7 to Eq. (1) as a function of the fragment mass. (a) results obtained from the curves referring to the light fragments; (b) and (c) results obtained from the curves referring to the heavy fragments.

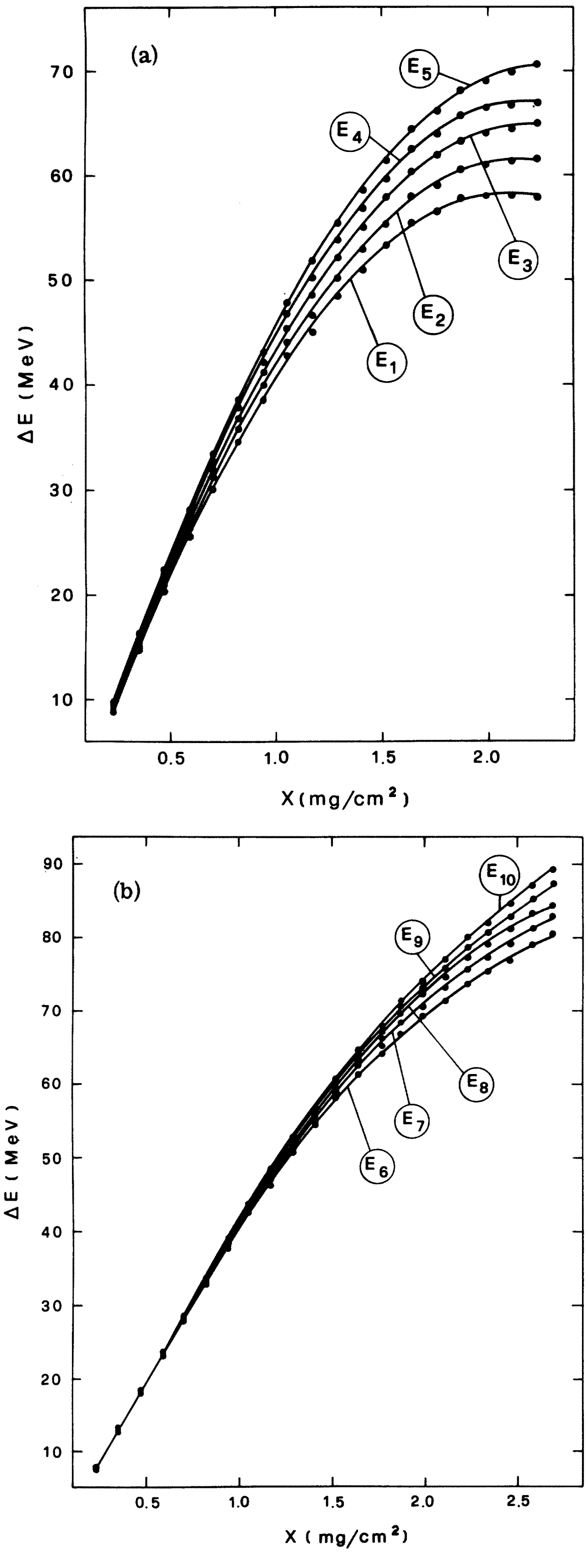

FIG. 9. Average energy loss (ΔE) of median-heavy (a) and median-light (b) fission fragments from ^{252}Cf having different initial energies (see for reference Tables VIII and IX).

TABLE VIII. Observed energy loss in argon [$\Delta E(x)$] for median-heavy (MH) fragments[a] having different observed initial kinetic energies $E_0 \pm 1$ MeV.

E_0 (MeV) symbol[b]	71.3 E_1	75.3 E_2	79.3 E_3	83.3 E_4	87.3 E_5
x (mg/cm^2)			$\Delta E(x)$ (MeV)		
0.23	8.9	9.1	9.4	9.6	9.8
0.35	14.7	15.1	15.5	15.9	16.3
0.47	20.4	21.0	21.6	22.0	22.4
0.59	25.6	26.4	27.1	27.7	28.1
0.70	30.1	31.3	32.0	32.8	33.5
0.82	34.6	35.8	36.9	37.9	38.6
0.94	38.6	40.0	41.2	42.2	43.2
1.05	42.8	44.1	45.4	46.9	47.9
1.17	45.1	46.7	48.6	50.3	51.9
1.29	48.5	50.3	52.2	53.9	55.5
1.41	51.0	53.0	55.1	56.9	58.7
1.52	53.4	55.4	58.0	59.7	61.5
1.64	55.5	57.9	60.4	62.5	64.5
1.76	56.6	59.1	62.0	64.0	66.2
1.87	57.8	60.5	63.3	65.7	68.1
1.99	58.1	61.0	64.0	66.5	69.1
2.11	58.1	61.4	64.5	66.7	69.5
2.23	58.0	61.6	65.0	68.0	70.8

[a] Selected mass interval: 141–143 amu.
[b] Quoted for reference to Fig. 9(a).

TABLE IX. Observed energy loss in argon [$\Delta E(x)$] for median-light (ML) fragments[a] having different observed initial kinetic energies $E_0 \pm 1$ MeV.

E_0 (MeV) symbol[b]	96.1 E_6	100.1 E_7	104.1 E_8	108.1 E_9	112.1 E_{10}
x (mg/cm^2)			$\Delta E(x)$ (MeV)		
0.23	7.5	7.7	7.7	7.7	7.8
0.35	12.7	12.8	12.9	13.0	13.2
0.47	18.1	18.3	18.5	18.5	18.5
0.59	23.2	23.3	23.5	23.6	23.6
0.70	27.9	28.2	28.3	28.6	28.6
0.82	33.0	33.2	33.4	33.6	33.8
0.94	37.7	38.0	38.2	39.0	39.1
1.05	42.6	43.0	43.4	43.6	43.8
1.17	46.4	47.3	47.8	48.2	48.6
1.29	50.9	51.4	51.9	52.3	52.7
1.41	54.6	55.3	55.8	56.6	56.9
1.52	58.3	59.0	59.4	60.5	60.8
1.64	61.5	62.7	63.5	64.3	64.8
1.76	64.3	65.4	66.4	67.3	68.1
1.87	67.0	68.6	69.7	70.7	71.5
1.99	69.4	70.7	72.5	73.3	74.2
2.11	71.5	73.3	74.7	76.0	77.1
2.23	73.7	75.7	77.4	78.7	80.3
2.34	75.5	77.4	79.2	80.9	82.2
2.46	77.1	79.3	81.6	83.0	84.8
2.58	79.1	81.3	83.4	85.4	87.3
2.69	80.6	83.0	84.5	87.5	89.4

[a] Selected mass interval: 105–107 amu.
[b] Quoted for reference to Fig. 9(b).

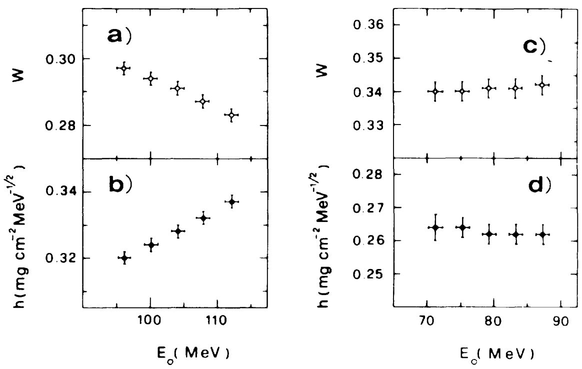

FIG. 10. Values of the parameters h and W obtained by fitting the range-energy curves in Fig. 9 to Eq. (1), as a function of the initial energy; (a) and (b): results referring to the ML fragments from ^{252}Cf; (c) results referring to the MH fragments from ^{252}Cf.

$$x = \text{const} \times \{[E_0 - \Delta E(x)]^{1/2} - (E_0)^{1/2}\}.$$

Furthermore, the values of h and W obtained in this way are coincident within the errors with those obtained from the preceding analysis (see Tables IV and VII).

One can then conclude that, dealing with fragments of the heavy group, h and W are independent both of the fragment mass and of the fragment initial energy. This means that, in the limit of the heaviest masses, the general dependence of the range-energy relation on the mass and nuclear charge of the interacting atoms is as predicted by the LSS Eqs. (1) and (2).

Concerning the ML fragments, the results prove that in this case the dependence of the energy loss

TABLE X. Values of the parameters h and W obtained by fitting the curves in Fig. 9 to Eq. (1). The errors on h and W are those supplied by the fitting procedure. (a) MH fragments; (b) ML fragments from ^{252}Cf.

Initial energy E_0 (MeV)	h (mg cm^{-2} MeV$^{-1/2}$)	W	χ^2/N_{DF}
	(a)		
71.3 ± 1.0	0.264 ± 0.004	0.340 ± 0.003	1.55
75.3 ± 1.0	0.264 ± 0.003	0.340 ± 0.003	1.62
79.3 ± 1.0	0.262 ± 0.003	0.341 ± 0.003	1.19
83.3 ± 1.0	0.262 ± 0.003	0.341 ± 0.003	0.99
87.3 ± 1.0	0.262 ± 0.003	0.342 ± 0.003	0.61
	(b)		
96.1 ± 1.0	0.320 ± 0.002	0.297 ± 0.002	2.26
100.1 ± 1.0	0.324 ± 0.002	0.294 ± 0.002	1.95
104.1 ± 1.0	0.328 ± 0.002	0.291 ± 0.002	1.25
108.1 ± 1.0	0.332 ± 0.002	0.287 ± 0.002	1.36
112.1 ± 1.0	0.337 ± 0.002	0.283 ± 0.002	1.09

on energy is somewhat different from the one foreseen by Eq. (1); in particular, the values found for the parameters h and W [which were previously shown to be remarkably mass dependent for the fragments of the light group (see Tables V and VII)] also turn out to be slightly dependent on the fragment initial kinetic energy.

IV. CONCLUSIONS

The results of a measurement of the energy loss in argon of fission fragments from ^{252}Cf have been presented, concerning that part of the range where electronic stopping power is dominant. The experiment has been performed by means of an apparatus which combines solid-state and gas-ionization chamber techniques, allowing one to determine the mass, the initial energy, and the energy lost in a given gaseous path for each detected fragment.

From the discussion reported in Sec. III, the following conclusions can now be drawn.

(i) In gaseous argon, the slowing down mechanism for fragments belonging to the heavy and light groups exhibits some different features, as is apparent from Figs. 7(a) and 7(b).

(ii) The dependence of the energy-loss characteristics on the mass of the moving fragments (on one hand) and on their initial kinetic energy (on the other) was determined separately by fitting the energy-loss curves (selected by suitable criteria, see Secs. III A–III C) to an expression of type (1). As a result of this procedure, it was found that in the case of the heavy fragments (i.e., $M \geq 135$ amu) the range-energy relations are faithfully described by Eq. (1) in the range where electronic stopping is certainly overwhelming with respect to nuclear stopping power. In particular, for such fragments and all their initial energies it was verified that h practically has a constant value. This is not the case for the fragments of the light group, for which the dependence of the energy loss on their mass, charge, and initial energy was found to be more complicated.

(iii) It is confirmed that the LSS theory can be simply modified in order to reproduce the experimental results on the energy loss of heavy fission fragments. For $M \geq 135$ amu, it was found that accurate predictions are obtained setting W in Eq. (1) to the value 0.34. For the case of the light fragments, the LSS theory cannot be applied even in this modified version, since the parameter W varies both with the fragment mass and with its initial energy.

A possible reason of the particular role of the heavy fragments with regard to the predictions of the LSS theory lies in the fact that they more safely fulfill the low-velocity conditions necessary for the validity of the LSS Eq. (1) than their light partners.

(iv) From a practical point of view, the results obtained for the parameter h (see Tables IV and VII) allow one to foresee the energy loss in argon for fragments having a known mass and initial energy, on the basis of Eq. (1), within the limits in which the variation of h with energy can be disregarded (see Table X). Furthermore, assuming that the explicit expression which the LSS [Eq. (2)] provides for h, is essentially correct, at least in the limit of the heaviest masses, the knowledge of this parameter could also be exploited to extract out the nuclear charge of the corresponding fragments, provided their masses are also measured.

ACKNOWLEDGMENTS

The authors are indebted to C. Maranzana and R. Valle for their skillful technical assistance. The Bologna group wishes to thank the Direction of the Centre Commun de Recherche Euratom (Ispra) for hospitality at the Center, the computer staff of Centro di Calcolo Interuniversitario, Bologna, for friendly assistance, Professor A. Alberigi Quaranta and Professor P. Bassi for their constant encouragement, and Professor A. Forino for useful discussions.

---

[1]See, e.g., E. Rutherford, *The Collected Papers of Lord Rutherford of Nelson* (Wiley, New York, 1962), Vols. I–III, and references therein.

[2]N. Bohr, Phys. Rev. 58, 654 (1940); 59, 270 (1941).

[3]L. C. Northcliffe, Ann. Rev. Nucl. Sci. 13, 67 (1963).

[4]H. A. Bethe, Ann. Phys. (Leipz.) 5, 325 (1930).

[5]F. Bloch, Ann. Phys. (Leipz.) 16, 285 (1933).

[6]H. D. Betz, Rev. Mod. Phys. 44, 465 (1972); M. D. Brown and C. D. Moak, Phys. Rev. B 6, 90 (1972); H. D. Betz, H. J. Isele, E. Rössli, and G. Hortig, Nucl. Instrum. Methods 123, 83 (1975).

[7]O. B. Firsov, Zh. Eksp. Teor. Fiz. 36, 1517 (1959) [Sov. Phys.-JETP 36, 1076 (1959)].

[8]J. Lindhard, M. Scharff, and H. E. Schiøtt, K. Dan. Vidensk. Selsk. Mat.-Fys. Medd. 33, 14 (1963); see also, J. Lindhard and M. Scharff, Phys. Rev. 124, 128 (1961).

[9]G. D. Sauter and S. D. Bloom, Phys. Rev. B 6, 699 (1972).

[10]N. K. Aras, M. P. Menon, and G. E. Gordon, Nucl. Phys. 69, 337 (1965); S. Hontzeas and H. Blok, Phys. Scr. 4, 229 (1971); H. Blok, F. M. Kiely, and B. D. Pate, Nucl. Instrum. Methods 100, 403 (1972); F. Demichelis, R. Liscia, and A. Tartaglia, Nuovo

Cimento B 10, 523 (1972).

[11]M. Forte, A. Bertin, M. Bruno, G. Vannini, and A. Vitale, Nuovo Cimento Lett. 4, 587 (1972); A. Bertin, M. Bruno, G. Vannini, A. Vitale, and M. Forte, Phys. Lett. A 43, 231 (1973).

[12]See, e.g., A. Bertin, M. Bruno, I. Massa, G. Vannini, and A. Vitale, Nuovo Cimento A 23, 185 (1974), and references therein.

[13]R. L. Watson, J. B. Wilhelmy, R. C. Jared, C. Rugge, H. R. Bowman, S. G. Thompson, and J. O. Rasmussen, Nucl. Phys. A 141, 449 (1970).

[14]J. B. Cumming and V. P. Crespo, Phys. Rev. 161, 287 (1967); S. Kahn and V. Forgue, Phys. Rev. 163, 290 (1967); V. Aiello, G. Maracci, and F. Rustichelli, Phys. Rev. B 4, 3812 (1971).

[15]N. O. Lassen, K. Dans. Videns. Sels. Mat.-Fys. Medd. 18, No. 11 (1949); H. W. Schmitt and R. B. Leachman, Phys. Rev. 102, 183 (1956); C. B. Fulmer, Phys. Rev. 108, 1113 (1957); F. Nasyrov, At. Eng. 16, 449 (1964) [Sov. Atom. Eng. 16, 552 (1964)]; G. B. Fulmer, Phys. Rev. 139, B54 (1965); P. M. Mulàs and R. C. Axtman, Phys. Rev. 146, 292 (1966); V. Forgue and S. Kahn, Nucl. Instrum. Meth. 48, 93 (1967); M. S. Moore and L. G. Miller, Phys. Rev. 157, 1049 (1967); M. Pickering and J. M. Alexander, Phys. Rev. C 6, 332 (1972).

[16]M. Forte, A. Bertin, M. Bruno, G. Vannini, and A. Vitale, Nucl. Instrum. Meth. 108, 525 (1973).

[17]B. V. Ershler and F. S. Lapteva, At. Eng. 1, 463 (1956) [J. Nucl. Energy, 4, 471 (1957)]; S. Pauker and N. H. Steiger-Shafrir, Nucl. Instrum. Meth. 91, 557 (1971).

[18]A standard mixture of argon with small nitrogen (2%) and buthane (3.5%) contaminations was used to fill the chamber.

[19]H. L. Adair, Nucl. Instrum. Meth. 100, 467 (1972).

[20]M. Forte, Proc. Colloque International sur l'Electronique Nucléaire, Versailles, 1968, p. 159 (unpublished).

[21]H. W. Schmitt, W. E. Kiker and C. W. Williams, Phys. Rev. 137, B837 (1965).

[22]H. R. Bowman, J. C. D. Milton, S. G. Thompson, and W. J. Swiatecki, Phys. Rev. 126, 2120 (1962); 129, 2133 (1963).

[23]J. Terrell, Phys. Rev. 127, 880 (1962).

[24]W. John, F. W. Guy, and J. J. Wesolowski, Phys. Rev. C 4, 1451 (1970).

[25]L. E. Glendenin and J. P. Unik, Phys. Rev. 140, B1301 (1965); W. Reisdorf, J. P. Unik, H. G. Griffin, and L. E. Glendenin, Nucl. Phys. A 177, 337 (1971); E. Cheifetz, J. B. Wilhelmy, R. C. Jared, and S. G. Thompson, Phys. Rev. C 4, 1913 (1971).